Article

Operator-Based Fractional-Order Nonlinear Robust Control for the Spiral Heat Exchanger Identified by Particle Swarm Optimization †

Guanqiang Dong and **Mingcong Deng** *

The Graduate School of Engineering, Tokyo University of Agriculture and Technology, Tokyo 184-8588, Japan
* Correspondence: deng@cc.tuat.ac.jp
† This paper is an extended version of our paper published in Proceedings of the 2021 International Conference on Advanced Mechatronic Systems under the title "Operator Based Fractional Order Control System for a Spiral Heat Exchanger with Uncertainties".

Abstract: Fractional-order calculus and derivative is extended from integral-order calculus and derivative. This paper investigates a nonlinear robust control problem using fractional order and operator theory. In order to improve the tracking performance and antidisturbance ability, operator- and fractional-order-based nonlinear robust control for the spiral counter-flow heat exchanger described by the parallel fractional-order model (PFOM) is proposed. The parallel fractional-order model for the spiral counter-flow heat exchanger was identified by particle swarm optimization (PSO) and the parameters of a fractional-order PID (FOPID) controller were optimized by the PSO. First, the parallel fractional-order mathematical model for a spiral counter-flow heat exchanger plant was identified by PSO. Second, a fractional-order PID controller and operator controller for the spiral heat exchanger were designed under the identified parallel fractional-order mathematical model. Third, the parameters of the operator and fractional-order PID were optimized by PSO. Then, tracking and antidisturbance performance of the control system were analyzed. Finally, comparisons of two control schemes were performed, and the effectiveness illustrated.

Keywords: system identification; parallel fractional model; fractional-order PID control; swarm particle optimization; right coprime factorization

1. Introduction

The first appearance of fractional-order calculus was in a letter from Leibniz in 1695 which expanded integral order calculus. However, fractional-order calculus has attracted great interest in the last several decades or so [1]. Some researchers have found that it allows them to present a real object more accurately than the conventional integer-order derivative and calculus in some fields such as the voltage–current relation of a semi-infinite lossy transmission line [2], economic systems [3], electric power systems [4], thermal systems [5], and the diffusion of heat through a semi-infinite solid, where heat flow is equal to the half-derivative of the temperature [6].

In real industries, proportional–integral–derivative(PID) control is considered to be the best control in the control system family for good control performance and robustness in linear or approximately linear systems [7]. By calculating and controlling three parameters—the proportional, integral, and derivative of how much a process variable deviates from the desired set point value—we can achieve different control actions for specific work. Therefore, the tuning of a PID controller's parameters is very important. Fractional-order PID (FOPID) control extended from the conventional PID control is extensively used by many scientists in order to achieve the most robust performance in control systems. The fractional PID controller was introduced by Podlubny, I. in 1994 for a fractional-order system [6]. A FOPID controller has five parameters to tune. Thus,

it is more flexible than a classical PID controller [8]. However, it is more difficult to tune. In references [9–12], different designs and tuning methods were presented. In this paper, different design methods along with available software tools and tuning methods are described. Basic definitions of fractional order are introduced with their use in control systems (or in engineering applications).

A spiral heat exchanger is widely used because it needs a smaller space for installation than traditional heat exchanger solutions and it has excellent heat transfer efficiency [13–15]. However, the spiral heat exchanger is a nonlinear system with uncertainties influenced by the input temperatures and flow rates of cold-fluid side and hot-fluid side, and other factors [16]. Therefore, it is difficult to control for the heated or cooled output temperature in variable working conditions.

Nonlinear robust control has been considered by many researchers in different methods in different fields [17–19]. In reference [20–22], the coprime right factorization was considered to compensate the nonlinearity of the system and the robust control performance of the system was improved. The coprime factorization is suited to not only linear feedback control but also nonlinear feedback control. It provides a convenient approach to study the input–output stability of nonlinear feedback control systems. The papers [23–26] studied the robust right coprime factorization of a nonlinear system with perturbations. A spiral heat exchanger mathematical model is described by integer differential equations in traditional methods. Reference [5] demonstrated a spiral heat exchanger mathematical model constructed by fractional differential equations was more accurate than traditional integer differential equations. In reference [27], Operator Based Fractional Order Control System for a spiral heat exchanger with uncertainties is proposed. However, the order of the fractional-order derivative was difficult to determine by a theoretical method, so the parameters of the fractional-order model were determined by a testing method. Therefore, motivated by the previous references, in order to improve its tracking performance and antidisturbance ability, an operator- and fractional-order-based nonlinear robust control for the spiral counter-flow heat exchanger described by a parallel fractional-order model (PFOM) is proposed. The parallel fractional-order model for the spiral counter-flow heat exchanger is identified by particle optimization (PSO) and the parameters of the fractional-order PID (FOPID) controller are optimized by PSO. A fractional-order PID controller and operator controller for the spiral heat exchanger are designed under the identified parallel fractional-order model. Comparisons of two control schemes are performed, and the effectiveness is illustrated.

The remainder of this paper is structured as follows. In Section 2, preliminaries and problem statement are presented. Section 3 introduces the parallel fractional-order model for the spiral counter-flow heat exchanger. The parallel fractional-order model for the spiral counter-flow heat exchanger is identified by PSO, with the least squares method as the performance index. In Section 4, operator- and fractional-order-based nonlinear robust control for the spiral counter-flow heat exchanger described by the identified parallel fractional-order model is proposed. Then, the parallel fractional-order operator controller and compensator are designed, with the compensator aiming to reduce disturbance. Section 5 optimizes the parameters of the fractional-order PID controller by PSO. Comparisons of two control schemes are performed to analyze the tracking and antidisturbance performance for the spiral counter-flow heat exchanger, and the effectiveness is verified in Section 6. Finally, a conclusion is given.

2. Preliminaries and Problem Statement

In this section, several definitions of fractional-order calculus, operator theory, and the modified swarm optimization are introduced.

2.1. The Definitions of Fractional Order

2.1.1. The Caputo Definition of Fractional Order

$$_a^C D_t^q y(t) = \frac{1}{\Gamma(n-q)} \int_a^t \frac{y^{(n)}(t)}{(t-\tau)} d\tau, n-1 \le q \le n \tag{1}$$

where $\Gamma(\cdot)$ is Gamma function defined by $\Gamma(\epsilon) = \int_0^\infty e^{-t} t^{\epsilon-1}$ and n is a positive integer number.

2.1.2. Grunwald–Letnikov's Definition of Fractional Order

$$_a^{GL} D_t^q y(t) = \lim_{h \to 0} h^{-q} \sum_{j=0}^{\left[\frac{t-a}{h}\right]} (-1)^j \frac{\Gamma(q+1)}{\Gamma(j+1)\Gamma(q-j+1)} y(t-jh) \tag{2}$$

where $[\cdot]$ means the integer part. (1) and (2) are equivalent if $y(\cdot)$ is differentiable. Grunwald–Letnikov's definition of fractional order is a discrete form of the fractional order definition, which is implemented easily on a CPU. Therefore, Grunwald–Letnikov's fractional order was used in this paper.

2.2. Particle Swarm Optimization

Particle swarm optimization (PSO) is a population-based stochastic optimization technique developed by Eberhart and Kennedy in 1995, inspired by the social behavior of bird flocking or fish schooling [28]. PSO shares many similarities with evolutionary computation techniques such as genetic algorithms (GA) and ant colony optimization (ACO) algorithms [29]. The system is initialized with a population of random solutions and searches for optima by updating iterations. However, unlike GA, PSO has no evolution operators such as crossover and mutation [30]. In PSO, potential solutions, called particles, fly through the problem space by following the current optimum particles.

It has been successfully applied to many problems in several fields such as biomedicine and energy conversion. Image analysis is one of the most frequent applications and it has been performed on biomedical images, microwave imaging, among others.

2.3. Operator Theory

In this section, operator theory is described. The robust stability analysis can be performed even with uncertainties that are difficult to model in mathematics. Here, a nonlinear control system with uncertainties can be designed in the time domain by operator theory and does not convert into the frequency domain by using a transfer function. A nonlinear feedback system based on operator theory is shown in Figure 1.
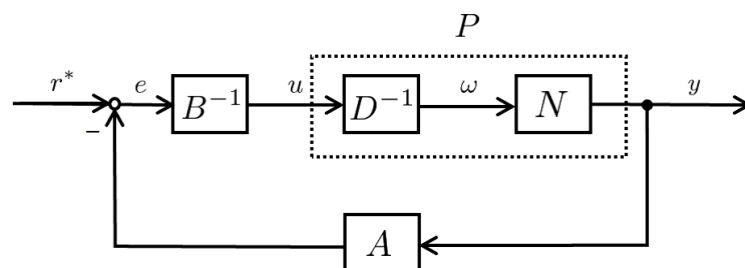

Figure 1. Nonlinear feedback system based on operator theory. Here, the plant P and operator controllers A, B^{-1} are nonlinear, r^* is the reference input signal.

2.3.1. Right Factorization

Let the plant be the operator $P : U \rightarrow Y : y(t) = P(u(t))$. If spaces U and Y of the input and output signals are two different extended linear spaces, plant P is unstable. A stable operator $N : w(t) \in W \rightarrow y(t) \in Y$ and stable operator $D : w(t) \in W \rightarrow u(t) \in U$ can be invertible. At this time, plant P is said to have a right factorization of N, D^{-1}.

$$P = ND^{-1} \tag{3}$$

2.3.2. Right Coprime Factorization

Suppose there is a right factorization operator N,D in plant P. The Bezout equation is obtained as follows.

$$AN + BD = M, \quad \forall M \in \mathcal{U}(W, U) \tag{4}$$

If a stable operator A and a stable and invertible operator B satisfies the above Bezout Equation (4), then plant P is said to have a right coprime factorization of A, B, N, and D as shown in Figure 2. The stability of the control system can be guaranteed.

2.3.3. Robust Right Coprime Factorization

In general, there are many uncertainties in an actual nonlinear control system that are difficult to express in a mathematical model. So, the stability of the nonlinear control system with uncertainties is no longer guaranteed. Therefore, by constructing a nonlinear feedback system with robust right coprime factorization, it is possible to analyze robust stability with uncertainties. The nonlinear feedback system with uncertainties is shown in Figure 2. Plant P without uncertainties is the nominal plant, and the actual plant with uncertainties ΔP is $\tilde{P} = P + \Delta P$.
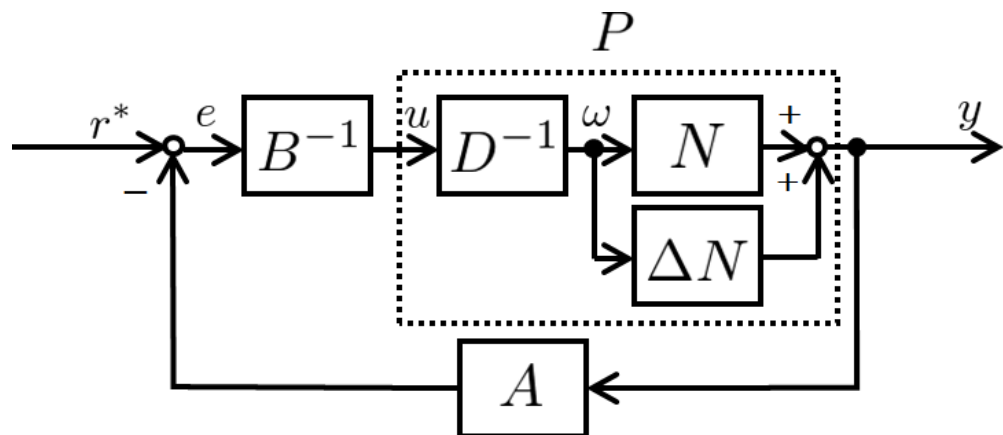

Figure 2. Nonlinear feedback control system with uncertainties. Here, the plant P is a nonlinear system with uncertainty ΔN, r^* is the reference input signal.

$$\tilde{P} = P + \Delta P = (N + \Delta N)D^{-1} \tag{5}$$

$$A(N + \Delta N) + BD = \tilde{M} \tag{6}$$

$$A(N + \Delta N) + BD = AN + BD = M \tag{7}$$

$$\|(A(N + \Delta N) - AN)M^{-1}\|_{Lip} < 1 \tag{8}$$

If the following inequality (8) is satisfied, $\tilde{M}$ is unimodular. In other words, the nonlinear feedback system with uncertainties can be said to have robust stability only if (8) is satisfied.

2.4. Statement Problem

A spiral heat exchanger is a nonlinear system with uncertainties. It is used widely in industry. In real application, the heated or cooled output temperature should track a timely reference input temperature in variable load conditions. However, the output temperature of the spiral heat exchanger is difficult to control for nonlinearity, uncertainties, and many disturbances. In conventional control methods, a PID controller is used to derive a good control performance in slow or no disturbances. In real application, there are many disturbances for the spiral heat exchanger, such as input temperature and flow rate on the hot-fluid side, input temperature on the cold-fluid side. Thus, due to the disturbances, control performance is poor in conventional control methods.

3. Fractional-Order System Identification for a Spiral Heat Exchanger by PSO

3.1. Parallel Fractional-Order Model for the Spiral Counter-Flow Heat Exchanger

3.1.1. Fractional-Order Model for the Spiral Counter-Flow Heat Exchanger

According to the law of heat energy balance of two fluids, the fractional-order derivative model for the spiral-plate counter-flow heat exchanger (See Appendix A) is derived as follows [31].

$$
\begin{cases}
D_\theta^{q_1} T_h(\theta,t) = \dfrac{(k+\Delta k)FAZ}{QL_1 c_h \rho_h}(T_c(\theta,t) - T_h(\theta,t)) \\[2mm]
D_\theta^{q_2} T_c(\theta,t) = \dfrac{(k+\Delta k)FAZ}{QL_2 c_c \rho_c}(T_h(\theta,t) - T_c(\theta,t)) \\[2mm]
\theta \in [0,11\pi]
\end{cases}
\tag{9}
$$

where $k = \frac{\delta_s}{\lambda}$, $k + \Delta k = \frac{1}{h_h} + \frac{\delta_s}{\lambda} + \frac{1}{h_c}$, $k_c = c_c \rho_c$, $k_h = c_h \rho_h$, and $\Delta T(\theta,t) = T_c(\theta,t) - T_h(\theta,t)$. $A = \sqrt{a^2 + b^2}$, and $A + \Delta A = \sqrt{a^2 + (b + a*11\pi)^2}$ $F \in [1,2]$, which is related to the plant of the spiral-plate heat exchanger. ρ_c, ρ_h are the densities of the cold fluid and the hot fluid, respectively. c_c, c_h are the specific heat capacities of the cold fluid and the hot fluid, respectively.

3.1.2. Parallel Fractional-Order Model for the Spiral Counter-Flow Heat Exchanger

The parallel fractional-order model for the spiral-plate counter-flow heat exchanger is described as follows.

$$
\begin{cases}
T_{hk} = (\Delta\theta)^{q_1} D_{hfrac} + B_h T_{hk-1} \\
T_{ck} = (\Delta\theta)^{q_2} D_{cfrac} + B_c T_{ck-1}
\end{cases}
\tag{10}
$$

where $T_{hk}, T_{hk-1}, D_{hfrac} \in R^N$, $B_h \in R^{N \times N}$, $T_{ck}, T_{ck-1}, D_{cfrac} \in R^N$, and $B_c \in R^{N \times N}$

$$
T_{hk} = \begin{pmatrix} T_h(\Delta\theta) \\ T_h(2(\Delta\theta)) \\ \vdots \\ T_h(N(\Delta\theta)) \end{pmatrix}
\tag{11}
$$

$$B_h = \begin{pmatrix} \frac{-\Gamma(q_1+1)}{\Gamma(2)\Gamma(q_1)} & 0 & \cdots & 0 \\ \frac{\Gamma(q_1+1)}{\Gamma(3)\Gamma(q_1-1)} & \frac{-\Gamma(q_1+1)}{\Gamma(2)\Gamma(q_1)} & \cdots & 0 \\ \vdots & \vdots & \vdots & \vdots \\ \frac{(-1)^N\Gamma(q_1+1)}{\Gamma(N+1)\Gamma(q_1-N+1)} & \frac{(-1)^{(N-1)}\Gamma(q_1+1)}{\Gamma(N)\Gamma((q_1-N+1)} & \cdots & \frac{-\Gamma(q_1+1)}{\Gamma(2)\Gamma(q_1)} \end{pmatrix} \tag{12}$$

$$T_{hk-1} = \begin{pmatrix} T_h(0) \\ T_h(\Delta\theta) \\ \vdots \\ T_h((N-1)(\Delta\theta)) \end{pmatrix} \tag{13}$$

$$B_c = \begin{pmatrix} \frac{-\Gamma(q_2+1)}{\Gamma(2)\Gamma(q_2)} & 0 & \cdots & 0 \\ \frac{\Gamma(q_2+1)}{\Gamma(3)\Gamma(q_2-1)} & \frac{-\Gamma(q_2+1)}{\Gamma(2)\Gamma(q_2)} & \cdots & 0 \\ \vdots & \vdots & \vdots & \vdots \\ \frac{(-1)^N\Gamma(q_2+1)}{\Gamma(N+1)\Gamma(q_2-N+1)} & \frac{(-1)^{(N-1)}\Gamma(q_2+1)}{\Gamma(N)\Gamma((q_2-N+1)} & \cdots & \frac{-\Gamma(q_2+1)}{\Gamma(2)\Gamma(q_2)} \end{pmatrix} \tag{14}$$

$$T_{ck} = \begin{pmatrix} T_c(\Delta\theta) \\ T_c(2\Delta\theta) \\ \vdots \\ T_c(N(\Delta\theta)) \end{pmatrix} \tag{15}$$

$$T_{ck-1} = \begin{pmatrix} T_c(0) \\ T_c(\Delta\theta) \\ \vdots \\ T_c((N-1)(\Delta\theta)) \end{pmatrix} \tag{16}$$

Therefore, the parallel fractional-order derivative model for the spiral-plate counter-flow heat exchanger is obtained.

$$\begin{cases} T_{hk} = (\Delta\theta)^{q_1}\dfrac{FkZA}{QL_1c_h\rho_h}(HT_{cK-1} - T_{hK-1}) + B_h T_{hk-1} \\ T_{ck} = (\Delta\theta)^{q_2}\dfrac{FkZA}{QL_2c_c\rho_c}(HT_{hK-1} - T_{cK-1}) + B_c T_{ck-1} \\ T_{cout} = CT_{ck} \end{cases} \tag{17}$$

where

$$H = \begin{pmatrix} 0 & 0 & 0 & \cdots & 0 & 1 \\ 0 & 0 & 0 & \cdots & 1 & 0 \\ \vdots & \vdots & \vdots & \vdots & \vdots & \vdots \\ 1 & 0 & 0 & \cdots & 0 & 0 \end{pmatrix} \tag{18}$$

$$C = \begin{pmatrix} 0 & 0 & 0 & 0 & \cdots & 1 \end{pmatrix} \tag{19}$$

where $C \in R^{1 \times N}$ and $H \in R^{N \times N}$. The parallel fractional-order model for the spiral counter-flow heat exchanger is a model with parallel input data.

3.2. Parallel Fractional-Order Model Identification for the Spiral Heat Exchanger

The schematic block of the parameter estimation for a parallel fractional-order model of the spiral counter-flow heat exchanger is shown in Figure 3.
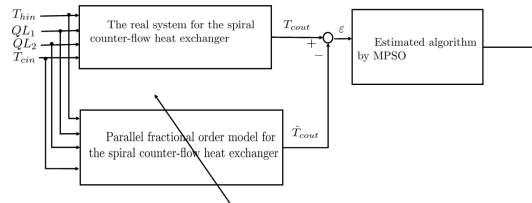

Figure 3. The schematic block of parameter estimation for the parallel fractional-order model of the spiral counter-flow heat exchanger.

The specific parameter estimation steps are follows.

(1) Determine the searched spaces for the estimated model.

Let $K_h = \dfrac{FkZA}{c_h \rho_h}$, $K_c = \dfrac{FkZA}{c_c \rho_c}$, then the parallel fractional-order model for the spiral counter-flow heat exchanger derived from (17) is the model's identified object as follows.

$$\begin{cases} T_{hk} = (\Delta\theta)^{q_1} \dfrac{K_h}{QL_1}(HT_{cK-1} - T_{hK-1}) + B_h T_{hk-1} \\ T_{ck} = (\Delta\theta)^{q_2} \dfrac{K_c}{QL_2}(HT_{hK-1} - T_{cK-1}) + B_c T_{ck-1} \\ T_{cout} = CT_{ck} \end{cases} \tag{20}$$

The researched space vector is defined as

$$x = \{q_1, q_2, K_h, K_c\} \tag{21}$$

where K_h, K_c are the model parameters and q_1, q_2 are the orders of the model. The range of the model parameter (K_h, K_c) was set to be [0 10], and the range of the model parameter (q_1, q_2) was set to be [0 2].

(2) Determine the performance index (evaluation function).

In this paper, the input flow rate of the hot-fluid side QL_1, the input flow rate of the cold-fluid side QL_2, the input temperature of the cold-fluid side T_{cin}, and the input temperature of the hot-fluid side T_{hin} were introduced as input signals of identified object. The sum of the squared errors between the output $\hat{T}_{cout}$ and the true value $\hat{T}_{cout}$,

$$J = \int_0^T [T_{cout}(t) - \hat{T}_{cout}(t)]^2 dt \tag{22}$$

was used as the performance evaluation function.

(3) The parameters of the algorithm are initialized to generate random search vectors.
(4) According to the steps of the PSO algorithm, the parameters in the parallel fractional-order model are identified.
(5) The iteration is repeated until the performance index is satisfactory or the sum of iterations go up to a maximum of 200.

The evolutionary curves of the estimated parameters are plotted in Figures 4–7.
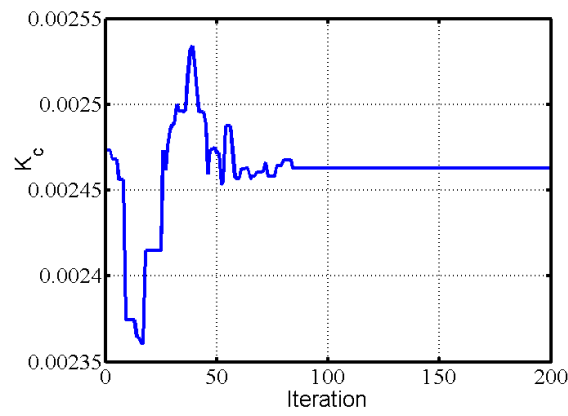
Figure 4. Evolutionary curve of the estimation of K_c.
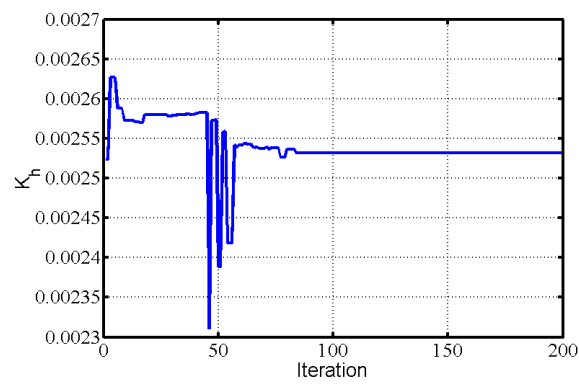

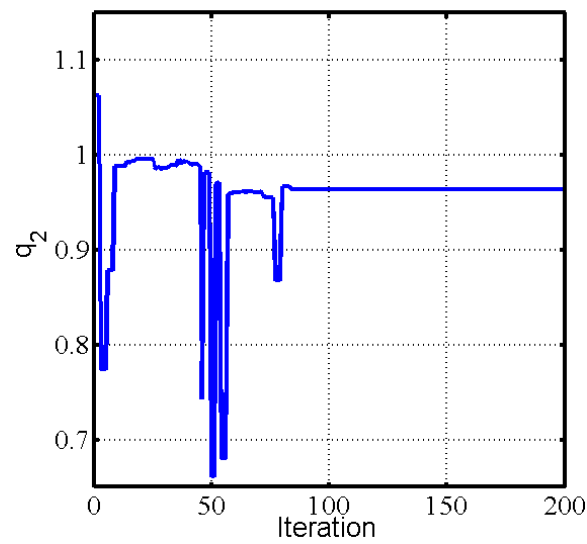**Figure 5.** Evolutionary curve of the estimation of K_h.

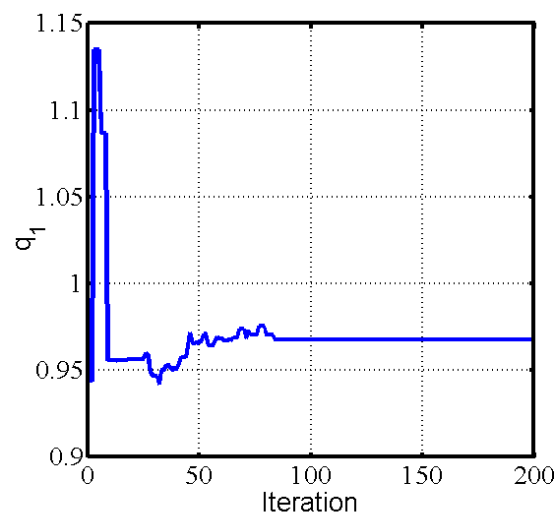**Figure 6.** Evolutionary curve of the estimation of q_2.

Figure 7. Evolutionary curve of the estimation of q_1.

The evolutionary curve of the performance index is plotted in Figure 8.
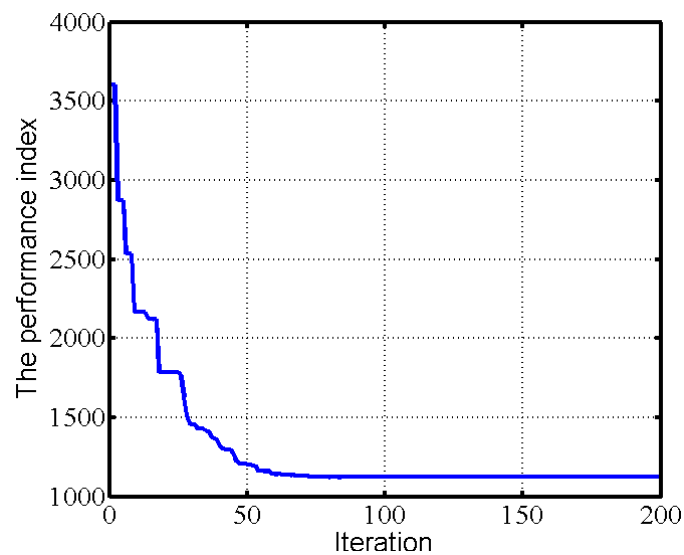

Figure 8. Evolutionary curve of the performance index.

The comparison of the output value from the identification system and the true value from the experiment is shown in Figure 9.
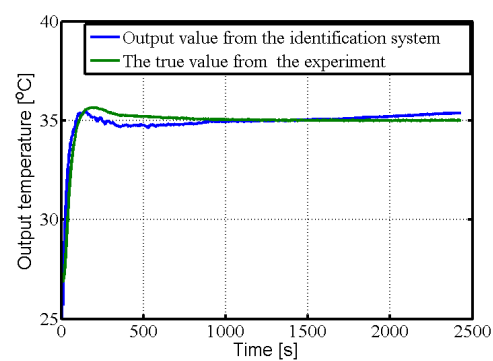

Figure 9. Comparison of the output value from the identification system and the true value from the experiment.

4. Operator-Based Fractional-Order PID Nonlinear Robust Control for the Spiral Heat Exchanger

In this section, two control schemes were designed in order to verify the tracking and antidisturbance performance of the operator-based fractional-order PID nonlinear robust control of the spiral heat exchanger, as shown Figures 10 and 11.
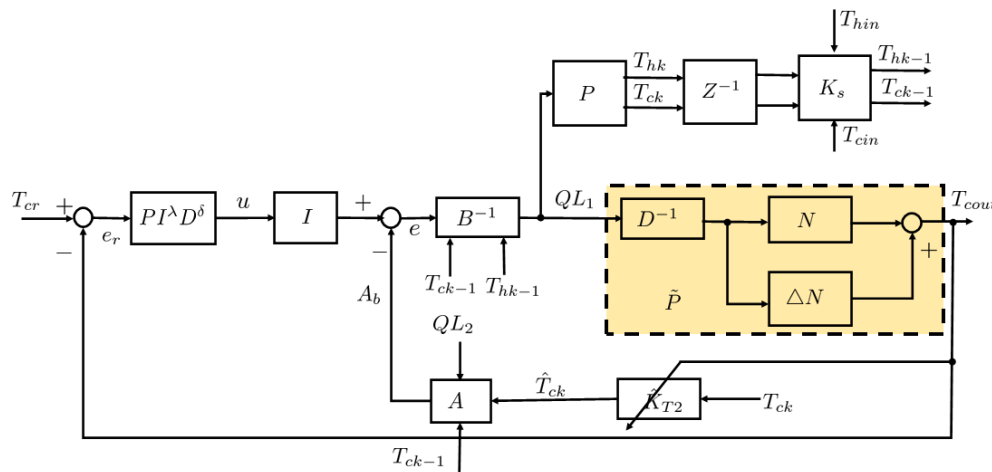

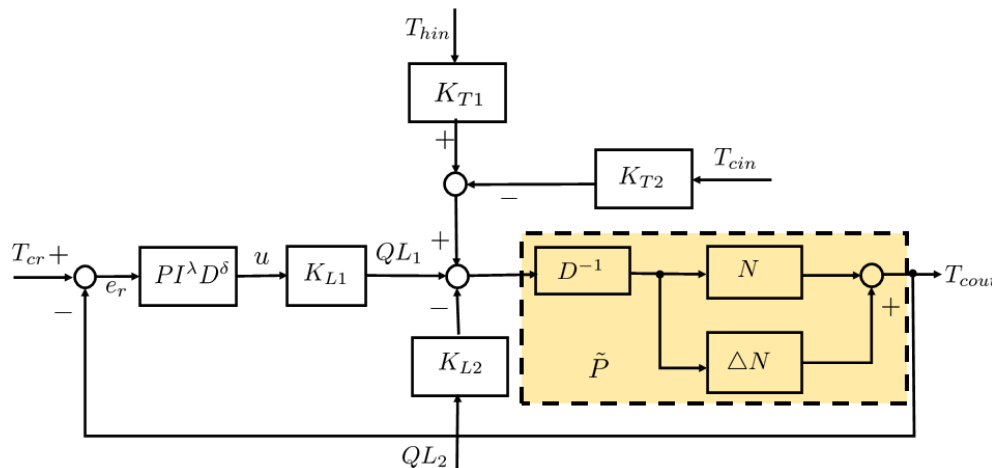**Figure 10.** FOPID controller with operator.

Figure 11. FOPID controller without operator.

4.1. Parallel Fractional-Order Model for the Spiral Heat Exchanger with Uncertainties

The heat transfer coefficient of the spiral heat exchanger plant $\tilde{k}$ is a relationship between not only the flow velocity of water, but also others. We know that the spiral heat exchanger model is nonlinear. Therefore, the spiral heat exchanger model is nonlinear system with uncertainties. The nonlinear fractional-order equations for the spiral heat exchanger model are described as follows.

$$
\begin{cases}
T_{hk} = (\Delta\theta)^{q_1} \dfrac{K_h}{QL_1}(HT_{cK-1} - T_{hK-1}) + B_h T_{hk-1} \\
T_{ck} = (\Delta\theta)^{q_2} \dfrac{K_c}{QL_2}(HT_{hK-1} - T_{cK-1}) + B_c T_{ck-1} \\
T_{cout} = CT_{ck}
\end{cases}
\tag{23}
$$

$$\begin{cases} T_{hk} = (\Delta\theta)^{q_1} \dfrac{(k+\Delta k)ZA_1}{QL_1 c_h \rho_h}(HT_{cK-1} - T_{hK-1}) + B_h T_{hk-1} \\ T_{ck} = (\Delta\theta)^{q_2} \dfrac{(k+\Delta k)ZA_2}{QL_2 c_c \rho_c}(HT_{hK-1} - T_{cK-1}) + B_c T_{ck-1} \\ T_{cout} = CT_{ck} \end{cases} \tag{24}$$

$$k = \frac{\delta_s}{\lambda} \tag{25}$$

where Δk are the uncertainties for the spiral heat exchanger.

4.2. Operator-Based Controller Design

In Figure 2, we show an operator nonlinear control system, where operators V and Y are the input and output spaces of this plant. Let (N, D) be the right factorization of P. The feedback nonlinear control system shown in Figure 2 is BIBO stable if there exist two stable operators A: Y → V, B: V → V (B is also invertible) satisfying Bezout's identity equation.

$$AN + BD = M \tag{26}$$

where M is a unimodular operator. Considering the uncertain term in the nonlinear system, with the designed operators A and B in Figure 2, the following equation could be satisfied.

$$\|A((N+\Delta N) - AN)M^{-1}\|_{Lip} < 1 \tag{27}$$

where $\| \bullet \|_{Lip}$ is a Lipschitz norm. Then, the nonlinear feedback control system has robust stability and M is a unimodular operator. The mathematical modeling $\tilde{P}$ considering the uncertain term ΔP can be given for the the spiral heat exchanger system as follows.

P :

$$\begin{cases} T_{hk} = (\Delta\theta)^{q_1} \dfrac{kZA_1}{QL_1 c_h \rho_h}(HT_{cK-1} - T_{hK-1}) + B_h T_{hk-1} \\ T_{ck} = (\Delta\theta)^{q_2} \dfrac{kZA_2}{QL_2 c_c \rho_c}(HT_{hK-1} - T_{cK-1}) + B_c T_{ck-1} \\ T_{cout} = CT_{ck} \end{cases} \tag{28}$$

K_s :

$$T_{hk-1} = \begin{pmatrix} 0 & 0 & \dots & 0 & 0 \\ 1 & 0 & \dots & 0 & 0 \\ 0 & 1 & \dots & 0 & 0 \\ \vdots & \vdots & \vdots & \vdots & \vdots \\ 0 & 0 & \dots & 1 & 0 \end{pmatrix} T_{hk} + \begin{pmatrix} 1 \\ 0 \\ 0 \\ \vdots \\ 0 \end{pmatrix} T_{hin} \tag{29}$$

$$T_{ck-1} = \begin{pmatrix} 0 & 0 & \dots & 0 & 0 \\ 1 & 0 & \dots & 0 & 0 \\ 0 & 1 & \dots & 0 & 0 \\ \vdots & \vdots & \vdots & \vdots & \vdots \\ 0 & 0 & \dots & 1 & 0 \end{pmatrix} T_{ck} + \begin{pmatrix} 1 \\ 0 \\ 0 \\ \vdots \\ 0 \end{pmatrix} T_{cin} \tag{30}$$

where Z^{-1} denotes a time delay of one sample period.

$P + \Delta P :$

$$\begin{cases} T_{hk} = (\Delta\theta)^{q_1} \dfrac{(k+\Delta k)ZA_1}{QL_1 c_h \rho_h}(HT_{cK-1} - T_{hK-1}) + B_h T_{hk-1} \\ T_{ck} = (\Delta\theta)^{q_2} \dfrac{(k+\Delta k)ZA_2}{QL_2 c_c \rho_c}(HT_{hK-1} - IT_{cK-1}) + B_c T_{ck-1} \\ T_{cout} = CT_{ck} \end{cases}$$

(31)

The plant can be right-coprime-factorized as follows.
$N + \Delta N : W \to Y$

$$T_{ck} = (\Delta\theta)^{q_2} \frac{(k+\Delta k)ZA_2}{QL_2 c_c \rho_c}(Hw - T_{cK-1}) + B_c T_{ck-1}$$

(32)

$D^{-1} : V \to W$

$$w = (\Delta\theta)^{q_1}\left(\frac{kA_1 Z}{QL_1 c_h \rho_h \delta_h}(HT_{cK-1} - T_{hK-1})\right) + B_h T_{hk-1}$$

(33)

The operator-based feedback control system is shown in Figure 10. The operators A and B were designed as follows.
$A : Y \to V$

$$b = (1 - K_p)H^{-1}\left[T_{ck-1} + \frac{QL_2 c_c \rho_c}{(\Delta\theta)^{q_2} ZkA_2}(\hat{T}_{ck} - B_c T_{ck-1})\right]$$

(34)

$$\hat{T}_{ck} = \frac{T_{cout}}{T_{ck}(end)}T_{ck}$$

(35)

$B^{-1} : V \to V$

$$QL_1 = (\Delta\theta)^{q_1} k_p \frac{ZkA_1(HT_{cK-1} - T_{hK-1})}{c_h \rho_h(e - B_h T_{hk-1})}$$

(36)

Operators A and B^{-1} were designed to satisfy the Bezout identity and k_p is the gain to be determined.

$$\|A((N + \Delta N) - AN)M^{-1}\|_{Lip} < 1$$

(37)

4.3. Fractional-Order Tracking Controller Design

The differential equation of fractional-order controller $PI^\lambda D^\delta$ is described as follows.

$$q(t) = K_{p1}e(t) + K_i D_t^{-\lambda}e(t) + K_d D_t^\delta e(t)$$

(38)

It is obvious that the fractional-order controller not only need three parameters K_{p1}, K_i, and K_d, but also two orders λ, δ of integral and derivative controller. The orders λ, δ are not necessarily integers, but any real numbers. As shown in Figure 12, the FOPID (fractional-order PID) controller generalizes the conventional integer-order PID controller and expands it from a point to a plane. This expansion could provide much more flexibility in PID controller design.
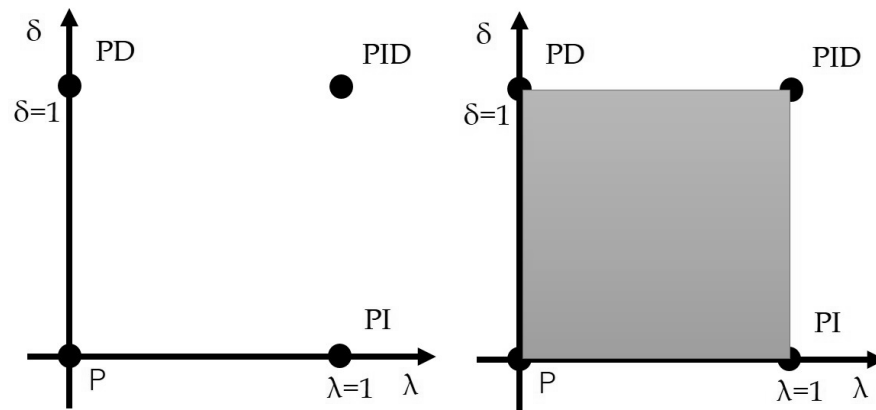
Figure 12. PID controller with the fractional orders.

5. Parameter Optima for Fractional-Order PID Controller

The specific parameter estimation steps were follows.

(1) Determine the searched spaces for the fractional-order PID controller.

The researched space vector was defined as

$$x = \{K_p, K_i, K_d, \lambda, \mu\} \tag{39}$$

where K_p, K_i, K_d are the gains and λ, μ are the orders. The range of the model parameter (K_p, K_i, K_d) was set to be [0 100], and the range of the model parameter (λ, μ) was set to be [0 1].

(2) Determine the performance index (evaluation function).

For determining the optimum values of the gains of the controller, the integral of time multiplied by the absolute value of the error (ITAE), the integral of the absolute value of the error (IAE), the integral of time multiplied by the squared error (ITSE), and the integral of the squared error (ISE) were taken as objective functions. The expression for these error functions are given below:

$$ITAE = \int_0^T t|T_{cr}(t) - T_{cout}(t)|dt \tag{40}$$

$$IAE = \int_0^T |T_{cr}(t) - T_{cout}(t)|dt \tag{41}$$

$$ITSE = \int_0^T t(T_{cr}(t) - T_{cout}(t))^2 dt \tag{42}$$

$$ISE = \int_0^T (T_{cr}(t) - T_{cout}(t))^2 dt \tag{43}$$

where T_{cout} is the output temperature, T_{cr} is the reference input temperature, and T is the time range of the simulation. In this paper, The ITSE was used as the performance evaluation function.

(3) The parameters of the algorithm are initialized to generate random search vectors.
(4) According to the steps of the PSO algorithm, the parameters of fractional-order PID controller are identified.
(5) The iteration is repeated until the performance index is satisfactory or the sum of iterations is maximal.

The evolutionary curves of the estimated parameters are plotted in Figures 13–16. The evolutionary curves of the performance index are plotted in Figures 17 and 18.
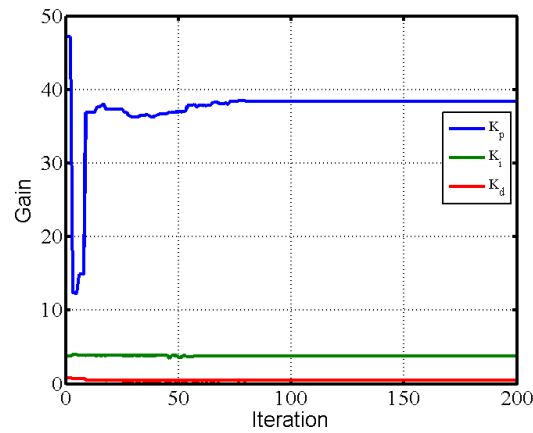

Figure 13. Evolutionary curve of estimated parameters (K_p, K_i, K_d) for FOPID controller with operator.
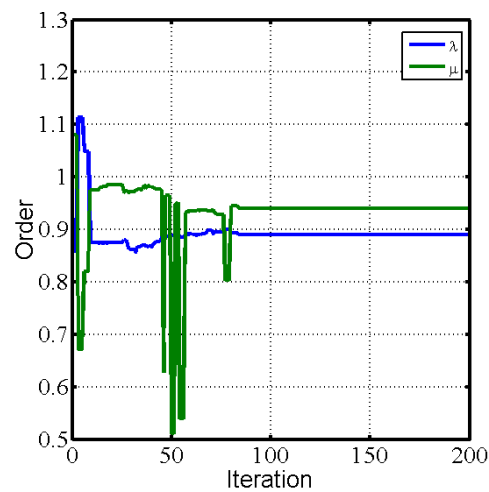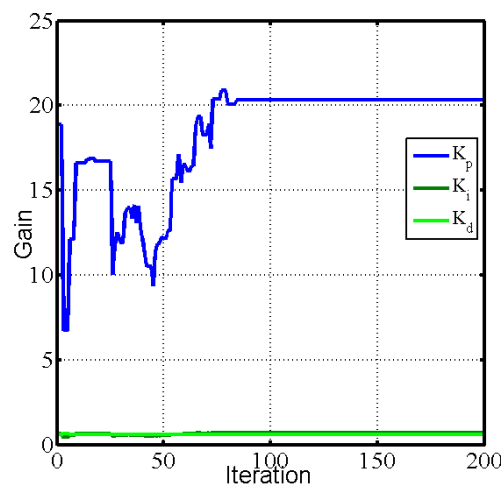

Figure 14. Evolutionary curve of estimated parameters (λ, μ) for FOPID controller with operator.

Figure 15. Evolutionary curve of estimated parameters (K_p, K_i, K_d) for FOPID controller without operator.
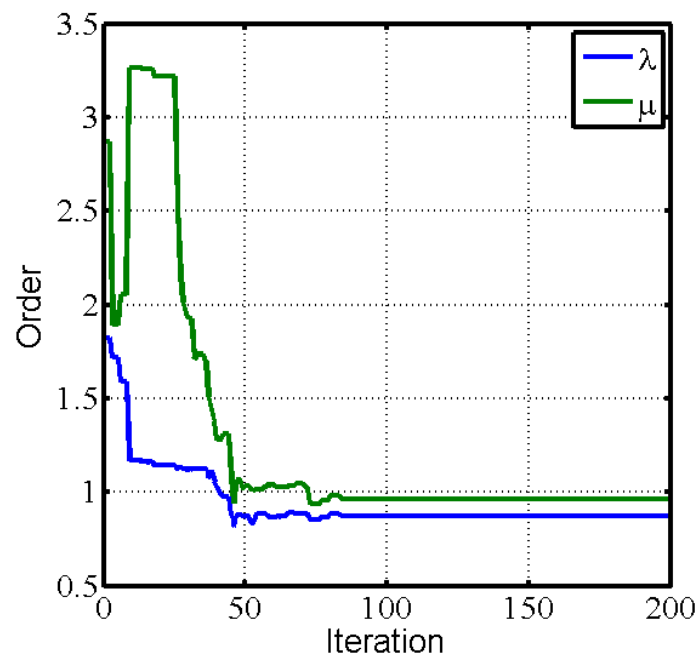
Figure 16. Evolutionary curve of estimated parameters (λ, μ) for FOPID controller without operator.
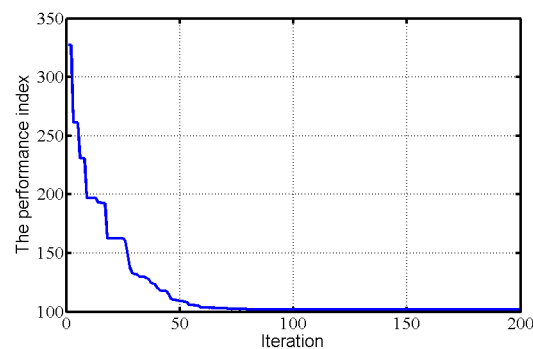

Figure 17. Evolutionary curve of the performance index for FOPID controller with operator.
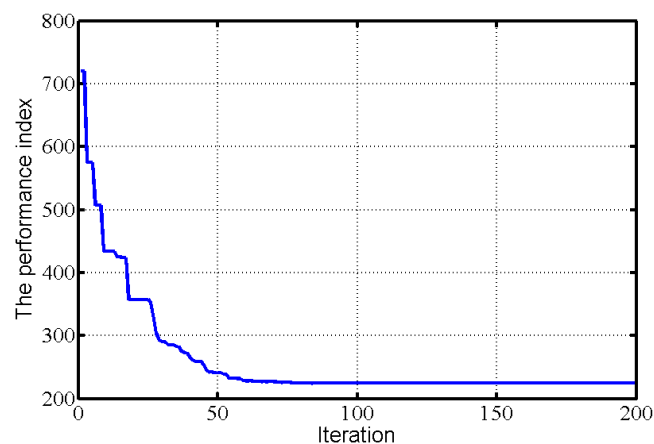

Figure 18. Evolutionary curve of the performance index for FOPID controller without operator.

6. Analysis of Performance on Tracking and Antidisturbances for the Spiral Heat Exchanger with Disturbances

In this section, the performance of the temperature control system for the spiral heat exchanger is analyzed. Two control schemes were simulated as shown in Figures 10 and 11.

6.1. Tracking Performance for the Spiral Heat Exchanger with Disturbances

In the simulation, a reference input signal T_r was decreased from 35 °C to 30 °C in 20 s; then, the reference input signal T_r was up to 35 °C. Figure 19 shows the operator-based fractional-order PID control scheme has better tracking performance than the fractional-order PID control scheme without operator. There is a small overshoot and a short settling time.
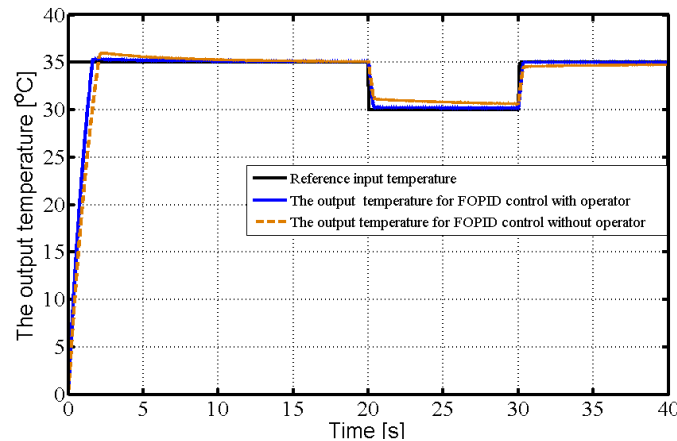

Figure 19. Tracking performance for the fractional-order spiral counter-flow heat exchanger.

6.2. Antidisturbance Performance for the Spiral Heat Exchanger

In real application, if the input flow rate of the hot-fluid side QL_1 is as control input, then the input temperature of the cold-fluid side T_{cin}, the input temperature of the hot-fluid side T_{hin}, and the input flow rate of the cold-fluid side QL_2 are three disturbances of the heat exchanger.

In the simulation, the disturbance signal T_{cin} was decreased from 20 °C to 15 °C in 20 s, T_{hin} was decreased from 50 °C to 45 °C in 20 s, and QL_1 was decreased from 5 L/Min to 3 L/Min in 20 s. Figures 20–22 show the operator-based fractional-order PID control scheme has better antidisturbance performance than the fractional-order PID control scheme without operator.
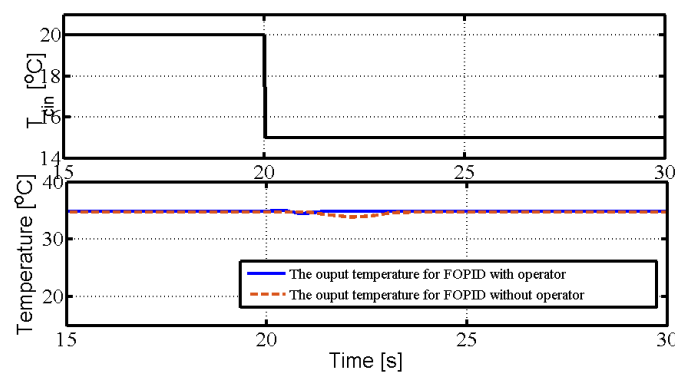

Figure 20. Antidisturbance performance to the input temperature of cold-fluid side.
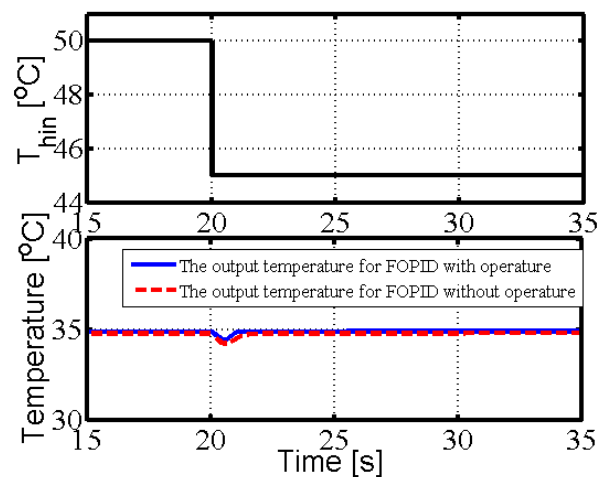
Figure 21. Antidisturbance performance to the input temperature of the hot-fluid side.
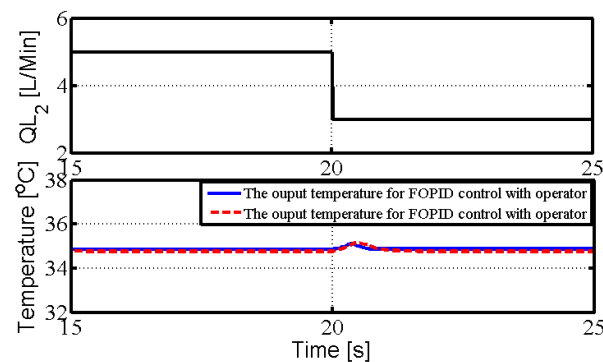

Figure 22. Antidisturbance performance to the input flow rate of cold-fluid side.

7. Conclusions

This paper proposed operator- and fractional-order-based nonlinear robust control for a spiral counter-flow heat exchanger described by a parallel fractional-order model in order to improve the tracking performance and antidisturbance ability. The parallel fractional-order model for the spiral counter-flow heat exchanger was identified by PSO and the parameters of the fractional-order PID controller were optimized by PSO. First, the parallel fractional-order mathematical model for the spiral heat exchanger plant was identified by PSO. Second, the operator controller for the spiral heat exchanger was designed under the identified parallel fractional-order model and a compensator was designed to reduce disturbance. Third, the parameters of the operator- and fractional-order-based PID controller were optimized by PSO. The tracking and antidisturbance performances of the control system were analyzed. Finally, comparisons of two control schemes were performed, and their effectiveness was illustrated.

Author Contributions: M.D. supervised the work; G.D. finished the simulation and wrote the rest of the work. All authors have read and agreed to the published version of the manuscript.

Appendix A. A Spiral Heat Exchanger Plant

A spiral-plate heat exchanger plant is shown in Figure A1. A spiral heat exchanger has many merits such as the ability to conduct a high-efficient heat exchange, a small size

compared to other heat exchangers, and having a self-cleaning action. As seen in Figure A2, a spiral heat exchanger has a spiral inner structure.

A heat spiral exchanger is an excellent process equipment, but it is difficult to obtain an accurate model due to a complex inner structure. Conventional methods such as the logarithmic mean temperature difference method, cannot obtain good control results. Another approach was conducted in [13], but the obtained model was too complex to design a controller based on the model. Therefore, this study introduced a new model for a spiral-plate heat exchanger to design the proposed controller. This modeling is one of our novelties. This section concretely explains the proposed method. Figure A2 shows the inner structure of the spiral-plate heat exchanger. In this study, the inner structure in Figure A2 was divided into a microvolume. The modeling considered the heat balance of the high temperature fluid and the low temperature fluid, respectively.

Figure A1. A spiral heat exchanger plant. Mini Spiral is a super compact spiral heat exchanger from Kurose Chemical Equipment Co., Ltd. in Japan. Design pressure is 0.6 MPaG. Design temperature is 185 °C. Material (JIS) is SUS316.
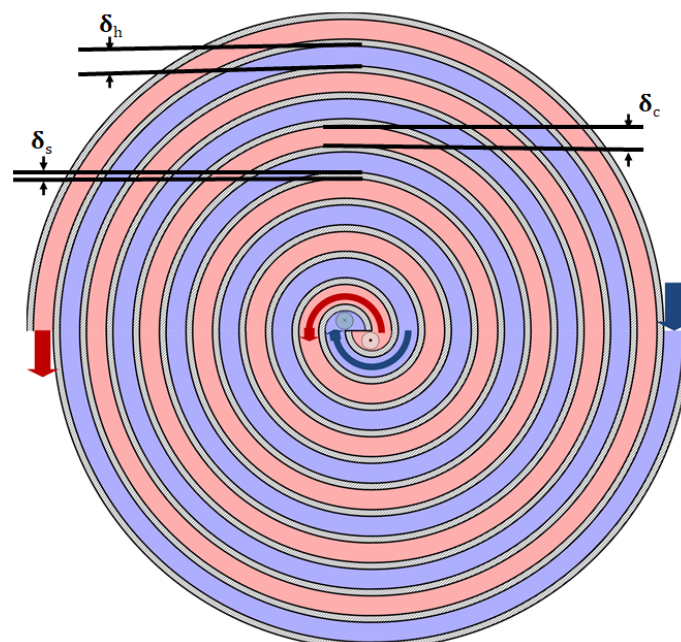

Figure A2. The inner structure for a spiral heat exchanger.

$$r = b - a \cdot \theta, \theta \in [0, 11\pi]$$ (A1)

The parameters of a spiral heat exchanger are denoted in Table A1.

Table A1. Parameters of a spiral heat exchanger.

Meaning (Symbol)	Value
Spiral function's parameter (a)	$\frac{0.005}{\pi}$ m/rad
Initial radius in high-temperature side (b)	0.08 m
Width of the flow channel (δ_h, δ_l)	0.005 m
Height of the spiral heat exchanger (Z)	0.011 m

References

1. Kilbas, S.G.; Kilbas, A.A. Marichev, O.I. *Fractional Integrals and Derivatives: Theory and Applications*; Gordon and Breach Science Publishers: Philadelphia, PA, USA, 1993.
2. Wang, J.C. Realizations of generalized warburg impedance with RC ladder networks and transmission lines. *J. Electrochem. Soc.* **1987**, *134*, 1915–1920. [CrossRef]
3. Laskin, N. Fractional market dynamics. *Phys. A Stat. Mech. Its Appl.* **2000**, *287*, 482–492. [CrossRef]
4. Ionescu, C.; Machado, J.T.; De Keyser, R. Fractional-order impulse response of the respiratory system. *Comput. Math. Appl.* **2011**, *62*, 845–854. [CrossRef]
5. Badri, V.; Tavazoei, M.S. Fractional order control of thermal systems: Achievability of frequency-domain requirements. *Nonlinear Dyn.* **2014**, *80*, 1773–1783. [CrossRef]
6. Podlubny, I. *Fractional Differential Equations*; Academic Press: San Diego, CA, USA, 1999.
7. Ang, K.H.; Chong, G.C.Y.; Li, Y. PID control system analysis, design, and technology. *IEEE Trans. Control. Syst. Technol.* **2005**, *13*, 559–576.
8. Tepljakov, A.; Baykant Alagoz, B.; Yeroglu, C. FOPID controllers and their industrial applications: A survey of recent results. *Int. J. Innov. Eng. Technol.* **2018**, *51*, 25–30.
9. Xue, D. *Fractional-Order Control Systems: Fundamentals and Numerical Implementations*; De Gruyter: Berlin, Germany, 2017.
10. Monje, C.A.; Vinagre, B.M.; Feliu, V.; Chen, Y. Tuning and auto-tuning of fractional order controllers for industry applications. *Control Eng. Pract.* **2008**, *16*, 798–812. [CrossRef]
11. Liu, L.; Tian, S.; Xue, D.; Zhang, T.; Chen, Y. Continuous fractional order Zero Phase Error Tracking Control. *ISA Trans.* **2018**, *75*, 226–235. [CrossRef]
12. Freeborn, T.J. A survey of fractional-order circuit models for biology and biomedicine. *IEEE J. Emerg. Andselected Top. Circuits Syst.* **2013**, *3*, 416–424. [CrossRef]
13. Tapre, R.W.; Kaware, J.P. Review on heat transfer in spiral heat exchanger. *Int. J. Sci. Res.* **2015**, *5*, 370–376.
14. Metta, V.R.; Konijeti, R.; Dasore, A. Thermal design of spiral plate heat exchanger through numerical modelling. *Int. J. Mech. Eng. Technol.* **2018**, *9*, 736–745.
15. Khorshidi, J.; Heidari, S. Design and construction of a spiral heat exchanger. *Adv. Chem. Eng. Sci.* **2016**, *6*, 201–208. [CrossRef]
16. Sathiyan, S.; Rangarajan, M. An experimental study of spiral-plate heat exchanger for nitrobenzene-water two-phase system. *Bulg. Chem. Commun.* **2010**, *42*, 205–209.
17. Liu, Z.; Sun, N.; Wu, Y.; Fang, Y. Nonlinear sliding mode tracking control of underactuated tower cranes. *Int. J. Control Autom. Syst.* **2021**, *19*, 1065–1077. [CrossRef]
18. Tuan, L.A. Neural observer and adaptive fractional-order backstepping fast-terminal sliding-mode control of RTG cranes. *IEEE Trans. Ind. Electron.* **2021**, *68*, 434–442. [CrossRef]
19. Shen, P.Y.; Schatz, J.; Caverly, R.J. Passivity-based adaptive trajectory control of an underactuated 3-DOF overhead crane. *Control Eng. Pract.* **2021**, *112*, 104834. [CrossRef]
20. Dong, G.; Deng, M. Operator & Fractional Order Based Nonlinear Robust Control for a Spiral Counter-flow Heat Exchanger with Uncertainties and Disturbances. *Machines* **2022**, *10*, 335.
21. Deng, M.; Wen, S.; Inoue, A. Operator-based robust nonlinear control for a Peltier actuated process. *Meas. Control J. Inst. Meas. Control* **2011**, *44*, 116–120. [CrossRef]
22. Wang, A.; Deng, M. Robust nonlinear multivariable tracking control design to a manipulator with unknown uncertainties using operator-based robust right coprime factorization. *Trans. Inst. Meas. Control* **2013**, *35*, 788–797. [CrossRef]
23. Wen, S.; Deng, M.; Inoue, A. Operator-based robust nonlinear control for gantry crane system with soft measurement of swing angle. *Int. J. Model. Identif. Control* **2012**, *16*, 86–96. [CrossRef]
24. Deng, M.; Inoue, A.; Soitiro Goto, G. Operator based thermal control of an aluminum plate with a Peltier device. *Int. J. Innov. Comput. Inf. Control* **2008**, *4*, 3219–3229.

25. Gao, X.; Deng, M. Tracking performance improvement for operator based nonlinear robust control of wireless power transfer systems with uncertainties. *Int. J. Control Autom. Syst.* **2019**, *17*, 545–554. [CrossRef]

26. Wu, Y.; Deng, M. Operator-based robust nonlinear optimal vibration control for an L-shaped arm driven by linear pulse motor. *Int. J. Control Autom. Syst.* **2017**, *15*, 2026–2033. [CrossRef]

27. Dong, G.; Deng, M. Operator Based Fractional Order Control System for a Spiral Heat Exchanger with Uncertainties. In Proceedings of the 2021 International Conference on Advanced Mechatronic Systems, Tokyo, Japan, 9–12 December 2021; pp. 242–247.

28. Kennedy, J.; Eberhart, R. Particle Swarm Optimization. In Proceedings of the ICNN'95—International Conference on Neural Networks, Perth, WA, Australia, 27 November–1 December 1995; pp. 1942–1948.

29. Pal, D.; Verma, P.; Gautam D.; Indait P. Improved optimization technique using hybrid ACO-PSO. In Proceedings of the 2016 2nd International Conference on Next Generation Computing Technologies, Dehradun, India, 14–16 October 2016; pp. 277–282.

30. Hendtlass, T. WoSP: A multi-optima particle swarm algorithm. In Proceedings of the IEEE Congress on Evolutionary Computation, Edinburgh, UK, 2–5 September 2005; pp. 727–734.

31. Dong, G.; Deng, M. GPU based modelling and analysis for parallel fractional order derivative model of the spiral-plate heat exchanger. *Axioms* **2021**, *10*, 344. [CrossRef]